

## MINIMIZATION OF VENTILATOR-INDUCED LUNG INJURY IN ARDS PATIENTS – PART I: COMPLEX MODEL OF MECHANICALLY VENTILATED ARDS LUNGS

Jarosław Glapiński, Ireneusz Jabłoński

Wrocław University of Science and Technology, Faculty of Electronics, Wybrzeże Wyspiańskiego 27, 50-370 Wrocław, Poland  
(✉ jaroslaw.glapinski@pwr.edu.pl, +48 71 320 6560, ireneusz.jablonski@pwr.edu.pl)

### Abstract

A complex model of mechanically ventilated ARDS lungs is proposed in the paper. This analogue is based on a combination of four components that describe breathing mechanics: morphology, mechanical properties of surfactant, tissue and chest wall characteristics. Physical-mathematical formulas attained from experimental data have been translated into their electrical equivalents and implemented in MultiSim software.

To examine the adequacy of the forward model to the properties and behaviour of mechanically ventilated lungs in patients with ARDS symptoms, several computer simulations have been performed and reported in the paper. Inhomogeneous characteristics observed in the physical properties of ARDS lungs were mapped in a multi-lobe model and the measured outputs were compared with the data from physiological reports. In this way clinicians and scientists can obtain the knowledge on the moment of airway zone reopening/closure expressed as a function of pressure, volume or even time. In the paper, these trends were assessed for inhomogeneous distributions (proper for ARDS) of surfactant properties and airway geometry in consecutive lung lobes.

The proposed model enables monitoring of temporal alveolar dynamics in successive lobes as well as those occurring at a higher level of lung structure organization, *i.e.* in a point  $P_0$  which can be used for collection of respiratory data during indirect management of recruitment/de-recruitment processes in ARDS lungs. The complex model and synthetic data generated for various parametrization scenarios make possible prospective studies on designing an indirect mode of alveolar zone management, *i.e.* with a minimized risk of repeated alveolar recruitment/de-recruitment and mechanical overstraining of lung tissues.

Keywords: lung alveolar surfactant, respiratory mechanics, mathematical modelling, medical decision support, lung protective ventilation.

© 2017 Polish Academy of Sciences. All rights reserved

### 1. Introduction

The clinical impact of *acute respiratory distress syndrome* (ARDS) and *acute lung injury* (ALI) is significant, with more than twenty thousand deaths per year [1]. There are reports which prove that improper mechanical ventilation of these patients can worsen ARDS mortality through a process of ventilator-induced lung injury [2]. What is more, it has been shown that lower tidal volumes and reduced plateau pressures led to a reduction of overall mortality [3]. However, a working point close to recruitment/de-recruitment phases brings a risk of repeated alveolar opening and collapse over time which contributes to further lung injury induced by ventilator [4–7].

One promoted strategy to prevent ventilator-induced lung injury is to open the lung and keep it open [8]. This scenario requires the recruitment manoeuvre to open the lung, followed by a sufficient *positive end-expiratory pressure* (PEEP) to maintain the lung in its newly open state [9]. There are numerous theoretical and experimental works devoted to studies of pressure and time dependencies as the fundamental contributors to undesirable repeatability of recruitment/de-recruitment actions [10–14]. But there is a lack of modelling studies which explain relationships between geometry of alveolar zone, surfactant characteristics and ARDS

lung mechanics expressed by pressure and flow trends recorded during mechanical ventilation, including consequences for optimal ventilation preserving repeated alveolar recruitment/de-recruitment.

Mathematical and physical-mathematical models of alveolar zone, which have been proposed in the literature [15], apply to respiratory mechanisms proper for breathing at volumes lower than the *total lung capacity* (TLC) [16–19]. The recruitment manoeuvre, especially in patients with ARDS or ALI (acute lung injury), is performed near and even above the TLC level. It means that the analogues reported in the literature are insufficient for reliable monitoring of alveolar conditions during recruitment of these structures over TLC. Additionally, logarithmic forms of models referenced in the literature [20] make impossible an easy description of peripheral lung mechanics at this volume level. Thus, replacing a logarithmic model with the polynomial one, which is well defined at/over TLC, and studying its properties and adequacy to the real conditions could be some kind of solution for this problem.

The paper presents a research program aimed at designing of a non-invasive procedure for monitoring of alveolar recruitment/de-recruitment based on pressure and flow signals measured at the mouth. Modelling of the respiratory system under mechanical ventilation is the first phase of this program. The proposed analogue, referenced to the experimental data, works near the TLC point and predicts mechanisms induced by surfactant properties during the recruitment manoeuvre in ARDS patients. The obtained results contribute to the understanding of complex interrelations occurring in ARDS lungs and signals generated in the model. Further, they can be used for designing an indirect measurement procedure for maintaining the working point of the lungs at the recruitment side of their pressure-volume characteristics, but close to the prevalent point located between the recruitment and the de-recruitment zones. Finally, minimization of the risk of repeated alveolar recruitment-de-recruitment and mechanical overstraining of lung tissues, at the same time, will result in limitation of lung injuries and their consequences, *i.e.* permanent and/or progressive limitation of the ventilation function.

## 2. Materials and methods

The proposed complex model of alveolar recruitment/de-recruitment is based on a combination of four elements that describe breathing mechanics: morphology, mechanical properties of surfactant, elasticity of tissue and the embedding of alveoli in the tissue (that is the connection with other alveoli via elastin and collagen fibres), and chest wall properties.

An alveolar pressure in static conditions can be described as the sum of pressures in consecutive structures of lung parenchyma, as it is shown in Fig. 1 and (1):

$$Palv = P_{\gamma} + Pt + Pcw + Pea, \quad (1)$$

where: *Palv* – an alveolar airway pressure; *P<sub>γ</sub>* – a surface tension pressure; *Pt* – a tissue pressure; *Pcw* – a rib cage and abdomen pressure; *Pea* – an external (ambient) pressure.

### 2.1. Modelling of alveolar geometry contribution in ventilated ARDS patients

A real shape of alveolar space in lung parenchyma is very complicated and unable to define [25]. Volume, thickness of alveoli wall, and microscopic anisotropy of expansion suggest a polyhedral shape of alveolus surface, but in many reports the shape of alveoli is assumed to be given by a simple geometrical model proposed to describe morphology properties [26, 27].

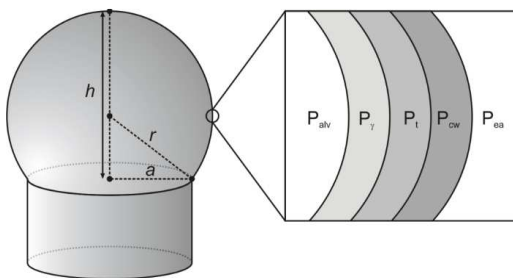


Fig. 1. Pressures defining equilibrium in the zone of alveoli;  $a$  – a diameter of the pulmonary bronchus;  $r$  – a diameter of the alveoli;  $h$  – a height of the alveoli.

For  $P_{alv} = 0$  a rigid ring forms a flat surface at the alveolar mouth. During inflation the fluid-air interface of the alveolus becomes a part of spherical shape and forms a saucer to almost spherical shape [28]. Using the geometrical relations, a surface tension pressure of the surfactant can be calculated from the approximation of shape of the bubble by the Laplace's law:

$$P_{\gamma} = \frac{2\gamma}{r}, \quad (2)$$

where:  $\gamma$  – a surface tension;  $r$  – an alveolus diameter.

A volume of alveolus ( $V_A$ ) can be calculated from the geometrical properties of a sphere shape:

$$V_A = \frac{1}{3}\pi h^2(3r - h), \quad (3)$$

$$r = \frac{a^2 + h^2}{2h}.$$

If we assume a ring diameter (for a normal human lung being from 50 to 150  $\mu\text{m}$ ) then changing the height of alveoli ( $h$ ) we can obtain the pressure-volume characteristics for the described model, as shown in Fig. 2.

The presented relationship between the surface tension pressure and the alveolar volume can be estimated by a function which well corresponds to the calculated data:

$$P_{\gamma} = \gamma * \frac{V_A + k_1}{k_2 * V_A^{k_3} + k_4} + k_5. \quad (4)$$

Values of coefficients  $k_1, \dots, k_5$  estimated for several ring diameters are presented in Table 1.

## 2.2. Analogue of mechanical properties of surfactant

The lung surfactant properties contribute significantly to the temporal status of lung mechanics. The lipid mixture covering all alveoli reduces the surface tension of air-liquid interface. This decreases the alveolar pressure during inflation and in consequence the amount of energy required to open the lung. Disorder in the surfactant amount or properties dependent on pathological changes can cause global pulmonary diseases, like a respiratory distress. The surfactant properties measured with the captive bubble surfactometry were described by Lu *et al.* [29]. The axisymmetric drop shape analysis and captive bubble technique were proposed to measure the mechanic properties of bovine lipid extract surfactant related to the bubble surface area. The results of observations show that an increase in the surface area of the bubble implies an increase in the surface tension, like shown in Fig. 3, from its minimum ( $\gamma_{min}$ ) to maximum value ( $\gamma_{max}$ ) [20].

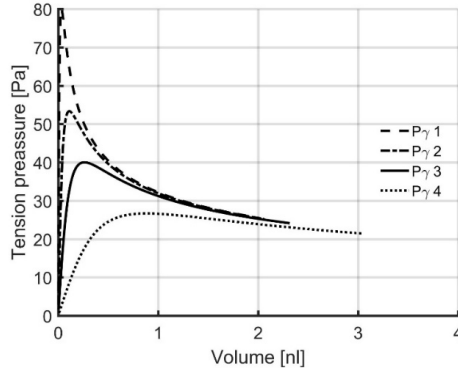


Fig. 2. Surface tension pressures ( $P_{\gamma i}$ ) related to the alveolar volume for ring diameters  $d_1 = 50$ ;  $d_2 = 75$ ;  $d_3 = 100$ ;  $d_4 = 150$  and  $\gamma = 1$ .

Table 1. Values of coefficients estimated with (4) for selected diameters of alveoli.

Parameter	Diameter of alveolus ( $r$ )			
	50 $\mu\text{m}$	75 $\mu\text{m}$	100 $\mu\text{m}$	150 $\mu\text{m}$
$k_1$	-0.013	-0.073	-0.24	-1.2
$k_2$	0.036	0.033	0.029	0.021
$k_3$	1.5	1.5	1.6	1.7
$k_4$	0.0021	0.012	0.039	0.21
$k_5$	5.2	5.8	6.0	5.60

It has been reported that in healthy human lungs the surface tension of surfactant is about 2–23 mN/m, whereas pathological processes can increase its value up to 73 mN/m (*i.e.* up to the plasma tension) and reduce the hysteresis properties [27]. The experimental relation between changes in the surface tension and changes in the surface area of surfactant were reported in the literature [30] and approximated by the equations:

$$\gamma = aA_R^2 + bA_R^2 + c, \quad A_R = \frac{A_A}{A_0}, \quad (5)$$

where:  $A_A$  – a relative surface area of alveolus at TLC;  $A_0$  – an alveolar surface at a reference level, and estimated coefficients:  $a = 98,9$  mN/m;  $b = -89.0$  mN/m;  $c = 18.3$  mN/m.

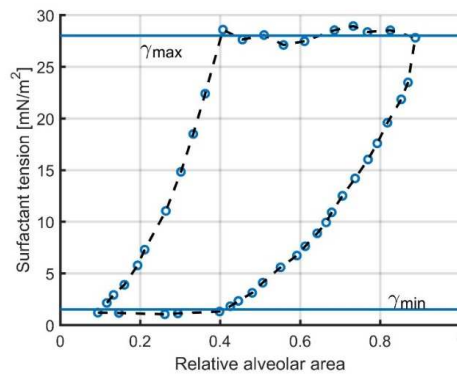


Fig. 3. The surfactant tension vs the relative alveolar area [29].

The hysteresis due to the properties of surfactant is caused by its structural transition from a mono- to multi-phase form and vice versa and is usually presented as the following function:

$$A_0 = \begin{cases} A_A & \text{if } 1 < A_R \\ A_0 & \text{if } A_{Meta} < A_R < 1, \\ A_A/A_{Meta} & \text{if } A_R < A_{Meta} \end{cases}, \quad (6)$$

where:  $A_{Meta}$  is a relative initial surface.

A relationship between the alveolar volume  $V_A$  and the surface area  $A_A$  was estimated by the polynomial function:

$$A_A = 0.56 * V_A^3 - 1.29 * V_A^2 + 1.73 * V_A^1. \quad (7)$$

Figure 4 shows relative changes of the alveolar area to TLC.

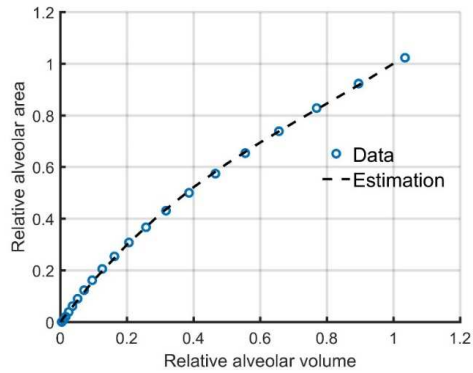


Fig. 4. The calculated dependence between relative changes in the alveolar area and in the alveolar volume.

### 2.3. Lung tissue model

Mechanical structures of lung parenchyma included in the model of lung tissue properties are described with the use of interpolation of the experimental results obtained during studies on animals [31]. This assessment is based on the equation by Andreassen [32]:

$$P_t = -\ln\left(\frac{V_{Arel}^{-1.01}}{-1.31} + 0.1909\right) * 0.4320 \text{ kPa}, \quad (8)$$

where  $V_{Arel}$  is an alveolar volume at TLC.

In the paper, the model of lung tissue properties is estimated by the equation:

$$P_t = V_{Arel}^{10} + 0,55 * V_{Arel} \text{ kPa}, \quad (9)$$

which has the best correlation with the measured data [31], as in Fig. 5.

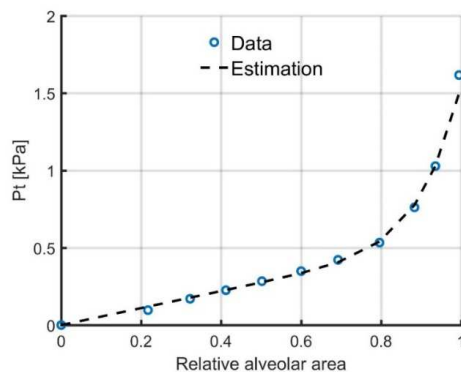


Fig. 5. A relationship between the elastic pressure and the relative volume of alveoli.

## 2.4. Chest wall model

A rib cage consists of curved ribs arranged in 12 pairs, ligaments and muscles, including the muscles between the ribs (intercostal muscles). These muscles on the one hand allow the ribcage to expand the lung while breathing, and to keep the negative intra-pleural pressure to prevent the alveoli to collapse while relaxation or sedation.

The chest wall properties were studied by Kimi Konno [33]. The oesophageal, gastric and mouth pressures were measured at different lung volumes during lung relaxation and with the closed mouthpiece. The presented data show the relationship between transthoracic and transabdominal pressures versus volume changes for standing and supine patient positions [34].

Steimle *et al.* proposed a mathematical description of the  $P_{cw}$  pressure dependent on the lung volume as the function [35]:

$$P_{cw} = 0.071 - \ln\left(\frac{95\%}{(V_{Atr}/V_{TLC})-22\%} - 1\right) * 0.58 \text{ kPa.} \quad (10)$$

This dependence was approximated by the following polynomial equation which enables modelling of the rib cage properties at volumes below 22% and over 100% of TLC (Fig. 6):

$$P_{cw} = 97,81 * V_{Arel}^5 - 339,89 * V_{Arel}^4 + 461,79 * V_{Arel}^3 - 306,13 * V_{Arel}^2 + 101,56 * V_{Arel}^1 - 13,59 \text{ kPa.} \quad (11)$$

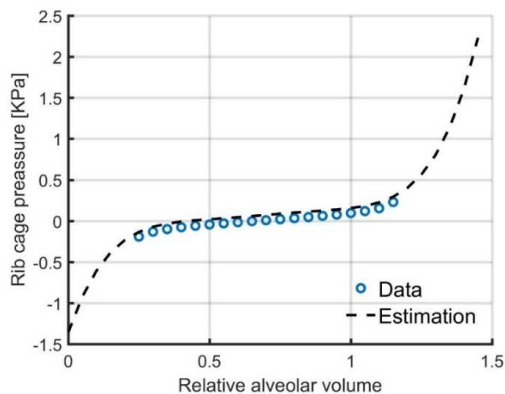


Fig. 6. A relationship between the rib cage pressure and the relative volume of alveoli.

## 2.5. Electrical model of lung recruitment in ARDS

The physical-mathematical model of ARDS lungs was translated into its electrical equivalent with the use of the electrical analogies and Multisim LabView software. An advantage of this approach and the programming tool is an easy implementation of electrical equivalents of physical systems, complex in structure and behaviour. What is more, for models described with a system of numerous differential equations the calculations are performed more efficiently in time [36, 37]. The proposed electrical equivalent suitable for imitation of lung recruitment/de-recruitment in a single lung lobe is presented in Fig. 7.

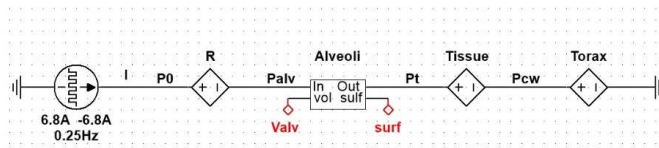


Fig. 7. An electrical forward model for simulation of lung recruitment/de-recruitment during ARDS in a single lobe.

$I$  corresponds to an airflow source of  $6,8 \text{ dm}^3/\text{s}$  amplitude, thus a simulation of 1 s duration enables to show pressure/volume dependencies for volumes from 0 to 100% of TLC and from TLC to 0.  $R$  module represents an airway resistance pressure drop with its temporal value equal to  $P_{res} = R \cdot I$ ,  $P_{alv}$  reconstructs an alveolar pressure drop as a function of volume ( $V_{alv}$ ) and temporal surfactant tension ( $surf$ ). The actual pressure ( $P_i$ ) caused by tissue properties is modelled with (9) and changes of the thorax pressure ( $P_{cw}$ ) are related to the thorax and abdomen properties, dependent on the lung volume (11).

The properties of surfactant hysteresis (Fig. 3) have been simplified to the alveolar area integration function (related to changes of the alveolar volume) with limits corresponded to the minimum ( $\gamma_{min}$ ) and maximum ( $\gamma_{max}$ ) values (Fig. 8).

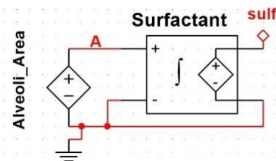


Fig. 8. An electrical equivalent of the simulation of mechanical properties of surfactant.

A challenge in management of the recruitment/de-recruitment process in ARDS lungs is the structural-parametric inhomogeneity. Thus, working with the analogues which implement this feature is fundamental for designing a reliable procedure of data processing during ARDS. The multi-compartment model of lungs from Fig. 9 addresses the defined demand. It enables to observe the pressure and flow signals at the mouth during recruitment/de-recruitment manoeuvres when different (e.g. inhomogeneous) parametric characteristics of lungs are implied in the successive branches.

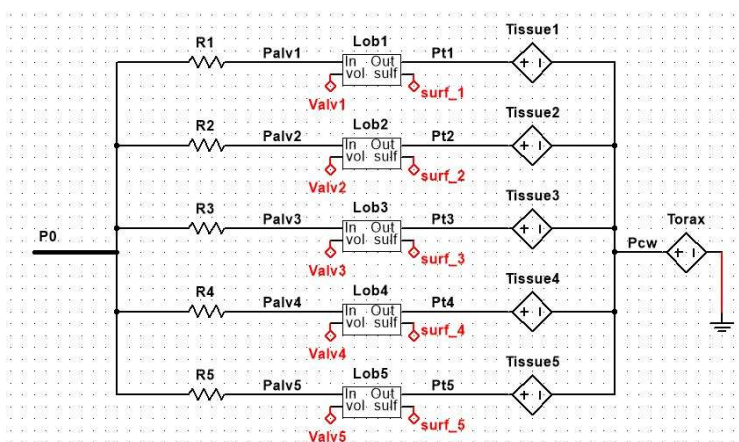


Fig. 9. A complex electrical forward model for simulation of lung recruitment/de-recruitment during ARDS.

In Fig. 9, each electrical branch simulates one lung lobe.  $TLC_i$  corresponds to the total capacity of  $i$ -th lobe, thus  $TLC = \sum_{i=1}^5 TLC_i$ .

ARDS patients need the ventilation support in order to improve and stabilize the exchange of respiratory gas [37]. There are numerous scenarios designed for an optimal ventilation regime [38, 39]. All these works are aimed at efficient control of the recruitment mechanism and minimizing lung injury during the long-term mechanical ventilation [40, 41]. To prove feasibility of the minimal invasive, indirect management of ARDS lung recruitment, a model of respirator was proposed, as in Fig. 10, and integrated in MultiSim with the forward analogue from Fig. 9.

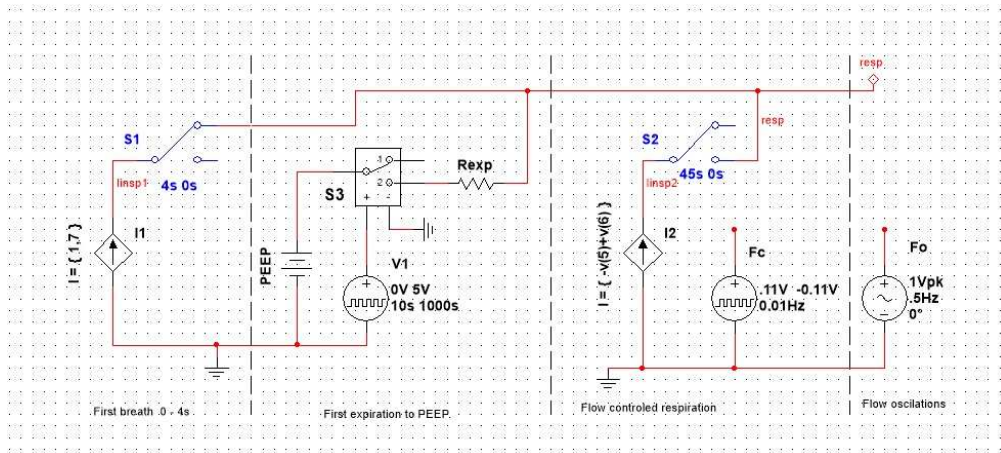


Fig. 10. An analogue of the respiratory signal of mechanical ventilation wave.

Its mode of operation assumes working as a generator of external excitation for the electrical equivalent of physiological system. Basically, a respiratory cycle comprises three phases in the designed model of respirator. Firstly, the lungs are filled with air in analogy to the first distending inspiration. To simulate this mechanism, the ventilation with a controlled flow (the airflow source  $I_1$ ) at a level of  $I_{insp1} = 1.7$  l/s was applied for a duration of 4s in order to achieve a respiratory volume equal to  $TLC = 6.8$  l. The spontaneous expiratory manoeuvre up to the *positive end-expiratory pressure* (PEEP) level was performed in the second phase. Finally, the steady breathing (inspiration and expiration) was simulated in the third phase of work of the respirator. In this phase, the ventilation with a controlled airflow ( $I_{insp2} = 0.011$  l/s) and a frequency (the pressure source  $F_c$ ) equal to 0.01 Hz was imitated, but the model enables also switching to the forced oscillation mode simulated by a source of sinusoidal wave excitation (the pressure source  $F_o$ ) generated with a frequency  $f_o = 0.5$  Hz.

### 3. Results

To examine the adequacy of the forward model to the properties and behaviour of mechanically ventilated lungs in patients with ARDS symptoms, several computer simulations have been performed and reported as below.

First of all, a model for the constant flow respiratory scenario was studied. Since the first breath was taken from 0 to 100% of TLC, the changes of alveolar airway pressure, surface tension pressure, surfactant properties, tissue pressure and rib cage and abdomen pressure due to the volume evolution were assessed. The simulations were performed for the structure from Fig. 9 where the parametric description assumes cooperation of four pathological lobes and one

physiological lobe in the respiratory system. More precisely, different diameters of alveolar rings ( $a = 50, 75, 100, 150 \mu\text{m}$ ) and a homogenous surfactant tension  $\gamma = 73 \text{ mN/m}$  were imitated in the pathological zone, whereas the parameter values in a single physiological lobe were set to  $a = 50 \mu\text{m}$  and  $\gamma = 2\text{-}23 \text{ mN/m}$ , respectively. The observations from Fig. 11 are in accordance with the data from physiological reports which prove that a decrease in size of alveolar rings for an increased level of  $\gamma$  leads to increasing surfactant pressure tensions in subsequent compartments [42]. It means that a higher recruitment pressure is required to reopen the alveolar zone with that pathological characteristic.

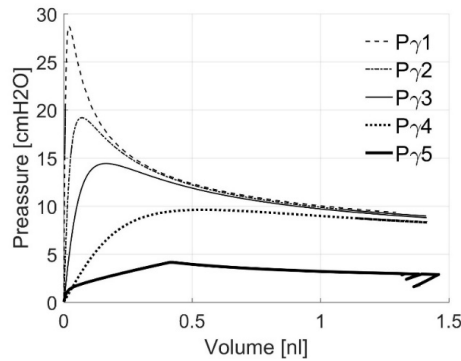


Fig. 11. The surfactant pressure tension related to the alveolar volume for lung lobes inhomogeneous in diameters ( $a$ ) and surfactant tensions ( $\gamma$ ).

An airway volume accessible for gas exchange in the alveolar space is also limited at the start of mechanical inflation of ARDS lungs (Fig. 12). In a healthy lung lobe  $V_{alv5}$  quickly inflates whereas for a pathological level of surfactant tension and the smallest alveolar ring  $a_1 = 50 \mu\text{m}$  the full capacity of alveoli  $V_{alv1}$  in the model of first lobe is available with a delay due to a larger shift in the recruitment moment. These shifts are clearly visible in Fig. 12 for consecutive lung lobes from the complex analogue – see trends for  $V_{alv1} - V_{alv4}$ .

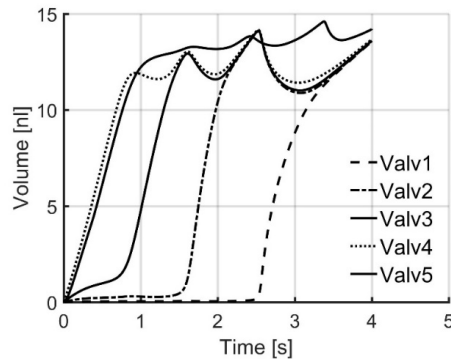


Fig. 12. Changes of volumes in successive lobes of the complex forward model of ARDS lungs.

For the clinicians involved in the management of lung recruitment/de-recruitment during the mechanical ventilation it is interesting to know the moment of airway zone reopening/closure expressed as a function of pressure, volume or even time [15]. Fig. 13 unveils this rule for alveolar pressures ( $P_{alv}$ ) measured in healthy and pathological lung zones of the complex forward model of ARDS lungs proposed in Section 2 (Fig. 9). An advantage of the presented

modelling approach is that the user can test the contribution of various scenarios of heterogeneous parametrization of the surfactant and the airway geometry to the pressure and/or volume responses. For example, for a given  $\gamma = 73$  mN/m, the pressure levels required to recruit the smallest three alveoli are the highest, and clear inflection points in trends  $P_{alv1} - P_{alv3}$ , apart from the moment of recruitment itself, show also the sensitivity of the model to the pendelluft between the compartments.

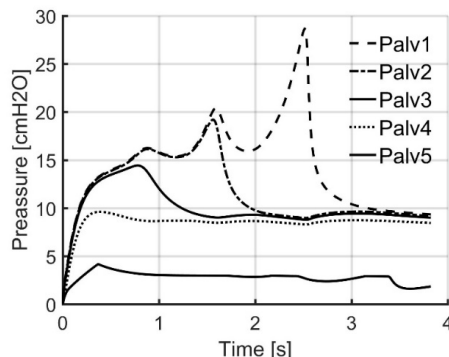


Fig. 13. Changes of pressures in successive lobes of the complex forward model of ARDS lungs.

A respiratory pressure ( $P_0$ ) is presented in Fig. 14. This is a level of inference selected in the research protocol as the access point for measurement of pressure and flow signals which can be used for the inverse model identification, *i.e.* for non-invasive monitoring of lung recruitment/de-recruitment. In other words, information on the occurrence of recruitment/de-recruitment is extracted here by estimation of changes in the lung elasticity (compliance).

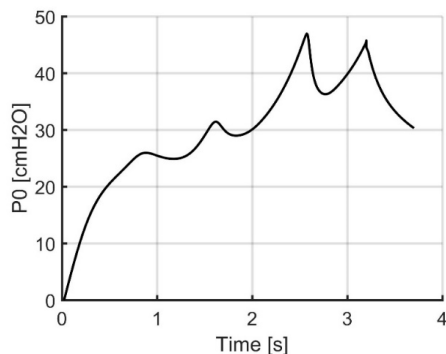


Fig. 14. Changes of pressure in the complex forward model of ARDS lungs.

The next stage of the forward model validation includes simulations of inspiration and expiration cycles in the analogue of mechanically ventilated ARDS lungs. In this phase of studies, the same value of airway ring diameter was applied in all lobes –  $a_{1,\dots,5} = 100$   $\mu\text{m}$ . The other parametrization was assumed in the forward equivalent to represent an inhomogeneous level of pathology in the surfactant properties, *i.e.* the values of surfactant tensions were equal to:  $\gamma_1 = 2\text{--}23$  mN/m,  $\gamma_2 = 10\text{--}23$  mN/m,  $\gamma_3 = 20\text{--}30$  mN/m,  $\gamma_4 = 40\text{--}60$  mN/m,  $\gamma_5 = 73\text{--}3$  mN/m, respectively. Changes of alveolar volumes ( $P_{alv}$ ) in successive lobes for reported conditions are shown in Fig. 15.

The observations are in agreement with the data from physiological reports, where for the homogeneous geometric conditions (the same diameters of airway rings) the availability of airway volume strongly depends on the surfactant tension  $\gamma$  [43, 44]. The higher  $\gamma$ , the higher the level of pathology, thus the greater shift in the moment of the airway recruitment expected. This is exactly the case proved in Fig. 15. What is more, the alveolar spaces in lobe 4 and lobe 5 are fully collapsed for some time during simulation.

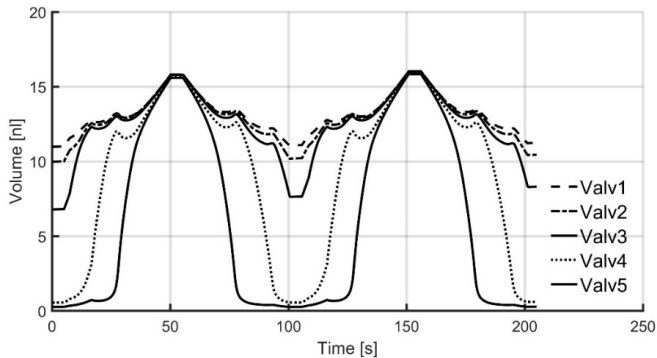


Fig. 15. Changes of volumes in successive lobes of the complex forward model of ARDS lungs during inspiration and expiration.

An inhomogeneous pathology in the surfactant tension ( $\gamma$ ) changes the balance of the surface forces during the alveolar reopening/closure. This implies an increase in the level of alveolar pressure at what the alveoli in all modelled lobes start to recruit and stay open, regardless of either constant (Fig. 16) or sinusoid wave excitation applied during the mechanical ventilation (Fig. 17).

In fact, numerous studies have shown that ventilation with a variable wave of complex content is closer to the physiological conditions, resulting in the limitation of lung injury during the artificial ventilation action [45, 46].

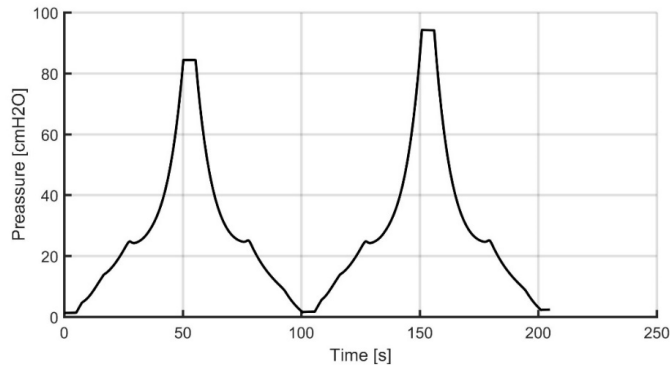


Fig. 16. A pressure response in the complex forward model of ARDS lungs during inspiration and expiration for a constant wave excitation.

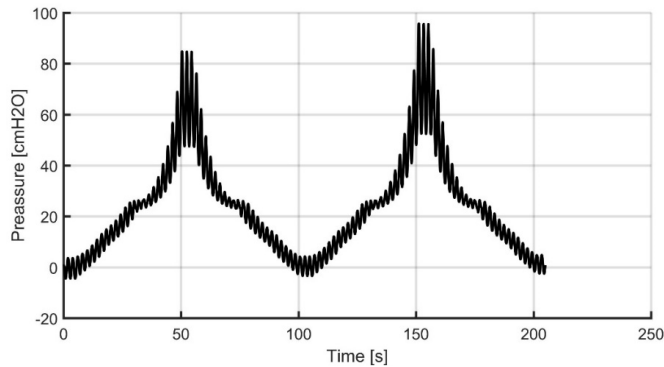


Fig. 17. A pressure response in the complex forward model of ARDS lungs during inspiration and expiration for a sinusoidal ( $f_{simus} = 0.5$  Hz) wave excitation.

#### 4. Summary

The paper initiates the work focused on designing of a procedure for monitoring of alveolar recruitment/de-recruitment in ARDS lungs and automatized, clinical supporting the system in a stable and optimized recruitment regime. The optimization concerns here the identification of a working point where ARDS lungs do not move repeatedly between the recruitment and de-recruitment states and do not experience a significant overstraining due to the working far from TLC, at the same time. The main problem identified in this topic is a lack of the simulation and the inverse model(s) suitable for quantitative characterization of processes occurring at the alveolar level with the use of signals measured at the airway opening. In fact, these complex and inverse modelling can work in tandem during designing a data processing algorithm for ARDS lung management, *i.e.* a forward-inverse experiment can be organized to contribute to the knowledge about the rules governing the recruitment/de-recruitment processes and their crosstalk visible at a higher level of lung structure organization, *e.g.* in  $P_0$  point (see Fig. 9). This is important since the clinical significance of the method requires non-invasive and thus indirect operation on a measured object. On the other hand, the clinical simplicity and usefulness of the final solution requires reliable operation on a limited amount of information and in the real-time mode.

The lung management of ARDS patients in clinical conditions has been carried out subjectively, *e.g.* based on observing characteristic levels in the output pressure and flow measured at the mouth and in the content of expiratory gas mixture. The primary goal is to identify and associate such characteristic features with physiological properties and to reconstruct the relations between the signals recorded at the airway opening and the processes measured in the alveolar space. Next, finding an algorithm of that mapping should be proposed in a real-time procedure for ARDS lungs.

A physical-mathematical forward model, including electrical equivalents, for the complex representation of processes and properties valid for ARDS lungs was proposed in the paper. This analogue includes a combination of four components that describe the breathing mechanics, *i.e.* ARDS lung morphology, mechanical properties of surfactant, tissue and chest wall characteristics. Here, especially the surfactant contribution to the observed output leads to the original inference into the temporal patterns of ARDS lungs' evolution during recruitment/de-recruitment. This was proved during the computer simulations for constant flow conditions and imitation of mechanical ventilation. It is possible to monitor pressure, flow and time dependencies during alveolar re-opening/closure processes using the complex model

described in the paper, both individually in distinguished lobes and at a level of their common output, e.g. a  $P_0$  point. The model was validated qualitatively, referring to the trend properties and levels measured in the complex electrical equivalent and reported in the literature. The multi-lobe analogue is able to reveal a contribution of parametric heterogeneity to the outputs recorded at various levels of the proposed model. These facts can be exploited when creating an algorithm of the task of automatized, clinical management of recruitment processes during mechanically supported breathing, leading to the limitation of further lung injuries in ARDS lungs.

The next stages of scheduled research include designing of an inverse, time-varying parameter model of ARDS lungs, building a procedure of inverse model identification, and validating the proposed approach during computer simulations and trials with the use of an anesthetized pig. From this point of view it is sufficient that the forward model reconstructs the most significant properties and trends observed in a real object, including the orders of values of measured signals and parameters. The results presented in Section 3 validate positively the usefulness of the complex analogue for prospective research. The quantitative results of accuracy assessment of the applied approach are confirmed in the next stages of work.

In summary, the proposed complex model of mechanically ventilated ARDS is a prerequisite for an adequate inverse modelling [47] and then for designing a procedure of lung recruitment with a minimized injurious impact on lung tissues. These steps will be delivered in the next paper, together with an example of the experimental measurement proving correctness of the modelling studies and feasibility of the method. In detail, apart from the computer simulations, the program of prospective research will include experimental work with the use of a mechanically induced lung injury animal model, under general anaesthesia during the mechanical ventilation.

## Acknowledgements

This work was supported by the National Science Centre under decision DEC-2013-11-B-ST7-01173.

## References

- [1] Rubenfeld, G.D. (2003). Epidemiology of acute lung injury. *Crit Care Med.*, 31, 276–284.
- [2] Dreyfuss, D., Saumon, G. (1998). Ventilator-induced lung injury: lessons from experimental studies. *Am J. Resp. Crit. Care Med.*, 157, 294–323.
- [3] Allen, G.B., Suratt, B.T., Rinaldi, L., Petty, J.M., Bates, J.H. (2006). Choosing the frequency of deep inflation in mice: balancing recruitment against ventilator-induced lung injury. *Am J. Physiol. Lung Cell Mol. Physiol.*, 291, L710–L717.
- [4] Slutsky, A.S. (1999). Lung injury caused by mechanical ventilation. *Chest*, 116, 9–15.
- [5] Hickling, K.G. (2001). Best compliance during a decremental, but not incremental, positive end-expiratory pressure trial is related to open-lung positive end-expiratory pressure: a mathematical model of acute respiratory distress syndrome lungs. *Am J. Respir. Crit. Care Med.*, 163, 69–78.
- [6] Hickling, K.G. (1998). The pressure-volume curve is greatly modified by recruitment. A mathematical model of ARDS lungs. *Am J. Respir. Crit. Care Med.*, 158, 194–202.
- [7] Pavone, L.A., Albert, S., Carney, D., Gatto, L.A., Halter, J.M., Nieman, G.F. (2007). Injurious mechanical ventilation in the normal lung causes a progressive pathologic change in dynamic alveolar mechanics. *Crit. Care*, 11, R64.
- [8] Lachmann, B. (1992). Open up the lung and keep the lung open. *Intensive Care Med.*, 18, 319–321.

- [9] Amato, M.B., Barbas, C.S., Medeiros, D.M., Magaldi, R.B., Schettino, G.P., Lorenzi-Filho, G., Kairalla, R.A., Deheinzelin, D., Munoz, C., Oliveira, R., Takagaki, T.Y., Carvalho, C.R. (1998). Effect of a protective-ventilation strategy on mortality in the acute respiratory distress syndrome. *N. Engl. J. Med.*, 338, 347–354.
- [10] Alencar, A.M., Buldyrev, S.V., Majumdar, A., Stanley, H.E., Suki, B. (2001). Avalanche dynamics of crackle sound in the lung. *Phys. Rev. Lett.*, 87, 088101.
- [11] Zhao, P., Yang, J., He, Y. (2017). Analysing the therapeutical action of lung recruitment maneuver on patients with acute respiratory distress syndrome by comparing different ventilation strategies. *Biomedical Research*, 28(4), 1828–1831.
- [12] Bates, J.H., Irvin, C.G. (2002). Time dependence of recruitment and derecruitment in the lung: a theoretical model. *J. Appl. Physiol. Respir. Environ. Exercise Physiol.*, 93, 705–713.
- [13] Brower, R.G., Morris, A., MacIntyre, N., Matthay, M.A., Hayden, D., Thompson, T., Clemmer, T., Lanken, P.N., Schoenfeld, D. (2003). Effects of recruitment maneuvers in patients with acute lung injury and acute respiratory distress syndrome ventilated with high positive end-expiratory pressure. *Crit. Care Med.*, 31, 2592–2597.
- [14] Meade, M.O., Cook, D.J., Guyatt, G.H., Slutsky, A.S., Arabi, Y.M., Cooper, D.J., Davies, A.R., Hand, L.E., Zhou, Q., Thabane, L., Austin, P., Lapinsky, S., Baxter, A., Russell, J., Skrobik, Y., Ronco, J.J., Stewart, T.E. (2008). Ventilation strategy using low tidal volumes, recruitment maneuvers, and high positive end-expiratory pressure for acute lung injury and acute respiratory distress syndrome: a randomized controlled trial. *JAMA*, 299, 637–645.
- [15] Albert, P., DiRocco, J., Allen, G.B., Bates, J.H.T., Lafollette, R., Kubiak, B.D., Fischer, J., Maroney, S., Nieman, G.F. (2009). The role of time and pressure on alveolar recruitment. *J. Appl. Physiol.*, 106, 757–765.
- [16] Ma, B., Bates, J.H.T. (2010). Modeling the complex dynamics of derecruitment in the lung. *Ann. Biomed. Eng.*, 38, 3466–3477.
- [17] Bates, J.H.T., Irvin, C.G. (2002). Time dependence of recruitment and derecruitment in the lung: A theoretical model. *J. Appl. Physiol.*, 93, 705–713.
- [18] DiRocco, J.D., Carney, D.E., Nieman, G.F. (2007). Correlation between alveolar recruitment/derecruitment and inflection points on the pressure-volume curve. *Intensive Care Med.*, 33, 1204–11.
- [19] Hickling, K.G. (1998). The pressure-volume curve is greatly modified by recruitment. A mathematical model of ARDS lungs. *Amer. J. Respir. Crit. Care Med.*, 158, 194–202.
- [20] Steimle, K.L., Mogensen, M.L., Karbing, D.S., de la Serna, J.B., Smith, B.W., Vacek, O., Andreassen, S. (2009). A Mathematical Physiological Model of the Pulmonary Ventilation. *Proc. of the 7th IFAC Symposium on Modelling and Control in Biomedical Systems Aalborg*, Denmark.
- [21] Lutchen, K.R., Costa, K.D. (1990). Physiological interpretations based on lumped element models fit to respiratory impedance data: use of forward-inverse modeling. *IEEE Transactions on Biomedical Engineering*, 37, 1076–1086.
- [22] Polak, A., Mrocza, J. (2006). Nonlinear model for mechanical ventilation of human lungs. *Comp. Biol. Med.*, 36(1), 41–58.
- [23] Polak, A. (2002). A Morphometric Model of Lung Mechanics for Time-Domain Analysis of Alveolar Pressures during Mechanical Ventilation. *Ann. Biomed. Eng.*, 30(4), 537–45.
- [24] Jabłoński, I., Mrocza, J. (2009). Frequency-domain identification of the respiratory system model during the interrupter experiment. *Measurement*, 42(3), 390–398.
- [25] Valberg, P.A., Brain, J.D. (1977). Lung surface tension and air space dimensions from multiple pressure-volume curves. *J. Appl. Physiol.*, 43, 730–738.
- [26] Sturm, R. (2015). A computer model for the simulation of nanoparticle deposition in the alveolar structures of the human lungs. *Annals of Translational Medicine*, 3(19).
- [27] Reifenrath, R. (1975). The significance of alveolar geometry and surface tension in the respiratory mechanics of the lung. *Respiration Physiology*, 24(2), 115–137.
- [28] Clements, J.A., Hustead, R.F., Johnson, R.P., Gribetz, I. (1961). Pulmonary surface tension and alveolar stability. *Journal of Applied Physiology*, 16(3), 444–450.

- [29] Lu, J.Y., Distefano, J., Philips, K., Chen, A.W. (1999). Neumann Effect of the compression ratio on properties of lung surfactant (bovine lipid extract surfactant) films. *Respiration Physiology*, 115, 55–71.
- [30] Sharp, J.T., Johnson, F.N., Goldberg, N.B., Van Lith, P. (1967). Hysteresis and stress adaptation in the human respiratory system. *J. Appl. Physiol.*, 23(4), 487–97.
- [31] Smith, J.C., Stamenovic, D. (1986). Surface forces in lungs. I. Alveolar surface tension-lung volume relationships. *J. Appl. Physiol.*, 60, 1351–1350.
- [32] Steimle, K.L., Mogensen, M.L., Karbing, D.S., Bernardino de la Serna, J., Andreassen, S. (2010). A model of ventilation of the healthy human lung. *Comput. Methods Programs Biomed.*, 101(2), 144–155.
- [33] Konno, K., Mead, J. (1968). Static volume–pressure characteristics of the rib cage and abdomen. *J. Appl. Physiol.*, 24(4), 544–548.
- [34] Goldman, M.D., Mead, J. (1973). Mechanical interaction between the diaphragm and rib cage. *Journal of Applied Physiology Published*, 35(2), 197–204.
- [35] Steimle, K.L., Mogensen, M.L., Karbing, D.S., Bernardino de la Serna, J., Andreassen, S. (2010). A model of ventilation of the healthy human lung. *Comput Methods Programs Biomed.*, 101(2), 144–55.
- [36] Jabłoński, I., Polak, A.G., Mrocza, J. (2011). A preliminary study on the accuracy of respiratory input interrupter measurement using the interrupter technique. *Computer Methods & Programs in Biomedicine*, 101(2), 115–125.
- [37] Jabłoński, I. (2013). Computer assessment of indirect insight during airflow interrupter maneuver of breathing. *Computer Methods & Programs in Biomedicine*, 110(3), 320–332.
- [38] Kretschmer, J., Wahl, A., Moller, K. (2011). Dynamically generated models for medical decision support systems. *Computers in Biology and Medicine*, 41, 899–907.
- [39] Malarkkan, N., Snook, N.J., Lumb, A.B. (2003). New aspects of ventilation in acute lung injury. *Anaesthesia*, 58(7), 627–728.
- [40] Amato, M.B., Barbas, C.S., Medeiros, D.M., Magaldi, R.B., Schettino, G.P., Lorenzi-Filho, G., Kairalla, R.A., Deheinzelin, D., Munoz, C., Oliveira, R., Takagaki, T.Y., Carvalho, C.R. (1998). Effect of a protective-ventilation strategy on mortality in the acute respiratory distress syndrome. *N. Engl. J. Med.*, 338, 347–354.
- [41] Putensen, C., Zech, S., Wrigge, H., Zinserling, J., Stuber, F., Spigel, T., Mutz, N. (2001). Long-Term Effects of Spontaneous Breathing During Ventilatory Support in Patients with Acute Lung Injury. *Am J. of Resp. and Critical Care Med.*, 164(1).
- [42] Harris, R.S.M. (2005). Pressure-Volume Curves of the Respiratory System. *Respiratory Care January*, 50(1).
- [43] Schoel, W., Schürch, S., Goerke, J. (1994). The captive bubble method for the evaluation of pulmonary surfactant: surface tension, area, and volume calculations. *Biochimica et Biophysica Acta (BBA) – General Subjects*, 1200(3), 281–290.
- [44] Schürch, S. (1982). Surface tension at low lung volumes: Dependence on time and alveolar size. *Respiration Physiology*, 48(3), 339–355.
- [45] Boker, A., Haberman, C.J., Girling, L., Guzman, R.P., Louridas, G., Tanner, J.R., Cheang, M., Maycher, B.W., Bell, D.D., Doak, G.J. (2004). Variable ventilation improves perioperative lung function in patients undergoing abdominal aortic aneurysmectomy. *Anesthesiology*, 100(3), 608–616.
- [46] Spieth, P., Carvalho, A., Pelosi, P., Hoehn, C., Meissner, C., Kasper, M., Hübler, M., von Neindorff, M., Dassow, C., Barrenschee, M., Uhlig, S., Koch, T., de Abreu, M.G. (2009). Variable Tidal Volumes Improve Lung Protective Ventilation Strategies in Experimental Lung Injury. *American Journal of Respiratory and Critical Care Medicine*, 179(8).
- [47] Mrocza, J., Szczuczyński, D. (2009). Inverse problems formulated in terms of first-kind fredholm integral equations in indirect measurements. *Metrol. Meas. Syst.*, 16(3), 333–357.